Elsevier Editorial System(tm) for Food Chemistry

Manuscript Draft

Manuscript Number: FOODCHEM-D-16-04593R1

Title: Unravelling the nanostructure of strawberry fruit pectins by endo-polygalacturonase digestion and atomic force microscopy

Article Type: Research Article (max 7,500 words)

Keywords: Atomic force microscopy; cell wall; Fragaria × ananassa; homogalacturonan; pectins; rhamnogalacturonan; strawberry

Corresponding Author: Dr. Jose A. Mercado,

Corresponding Author's Institution: Universidad de Malaga

First Author: Candelas Paniagua

Order of Authors: Candelas Paniagua; Andrew R. Kirby; A. Patrick Gunning; Victor J Morris; Antonio J Matas; Miguel A. Quesada; Jose A. Mercado

Abstract: Pectins analysed by AFM are visualized as individual chains, branched or unbranched, and aggregates. To investigate the nature of these structures, sodium carbonate soluble pectins from strawberry fruits were digested with endo-Polygalacturonase M2 from Aspergillus aculeatus and visualized by AFM. A gradual decrease in the length of chains was observed as result of the treatment, reaching a minimum LN value of 22 nm. Branches were not visible after 2h of digestion. The size of complexes also diminished significantly with the enzymatic digestion. A treatment to hydrolyse rhamnogalacturonan II borate diester bonds neither affected chains length or branching nor complex size but reduced the density of aggregates. These results suggest that chains are formed by a mixture of homogalacturonan and more complex molecules composed by a homogalacturonan unit linked to an endo-PG resistant unit. Homogalacturonan is a structural component of the complexes and rhamnogalacturonan II could be involved in their formation

December 14, 2016

Dear Editor

Please, find enclosed the revised version of our ms no. FOODCHEM-D-16-04593 and our answers to the reviewer`s concerns. Main changes made in the manuscript are labelled in red.

Looking forward to hearing from you

Yours sincerely

José A. Mercado
Dep. Biología Vegetal
Universidad de Málaga
29071, Málaga, Spain

Highlights:

1. Strawberry fruit pectins are visualized by AFM as linear chains and large complexes

2. Digestion with fungal endoPG reduces the size of linear chains and complexes

3. An acid treatment to eliminate RGII dimers diminishes the number of complexes

4. Pectin chains are formed by a mixture of HG and HG linked to an endoPG resistant unit

5. RGII dimers are involved in the formation of the pectin complexes

*Manuscript
Click here to download Manuscript: Paniagua-Revised.docx Click here to view linked References

Unravelling the nanostructure of strawberry fruit pectins by endo-polygalacturonase digestion and atomic force microscopy

Candelas Paniagua [a], Andrew R. Kirby [b], A. Patrick Gunning [b], Victor J. Morris[b], Antonio J. Matas[a], Miguel A. Quesada [c], José A. Mercado[a*]

[a]Instituto de Hortofruticultura Subtropical y Mediterránea "La Mayora" (IHSM-UMA-CSIC), Departamento de Biología Vegetal, Universidad de Málaga, 29071, Málaga, Spain.

[b] Institute of Food Research, Norwich Research Park, Colney, Norwich, NR4 7UA, UK.

[c]Departamento de Biología Vegetal, Universidad de Málaga, 29071, Málaga, Spain.

*Corresponding author.

E-mail: mercado@uma.es (Jose A. Mercado)

Corresponding author:

José A. Mercado

Instituto de Hortofruticultura Subtropical y Mediterránea "La Mayora" (IHSM-UMA-CSIC), Dept. de Biología Vegetal, Universidad de Málaga, 29071, Málaga, Spain

e-mail: mercado@uma.es

Fax: +34 952 13 20 00

Abstract

Pectins analysed by AFM are visualized as individual chains, branched or unbranched, and aggregates. To investigate the nature of these structures, sodium carbonate soluble pectins from strawberry fruits were digested with endo-Polygalacturonase M2 from *Aspergillus aculeatus* and visualized by AFM. A gradual decrease in the length of chains was observed as result of the treatment, reaching a minimum L_N value of 22 nm. The branches were not visible after 2 h of enzymatic incubation. The size of complexes also diminished significantly with the enzymatic digestion. A treatment to hydrolyse rhamnogalacturonan II borate diester bonds neither affected chains length or branching nor complex size but reduced the density of aggregates. These results suggest that chains are formed by a mixture of homogalacturonan and more complex molecules composed by a homogalacturonan unit linked to an endo-PG resistant unit. Homogalacturonan is a structural component of the complexes and rhamnogalacturonan II could be involved in their formation.

Keywords: Atomic force microscopy, cell wall, *Fragaria* × *ananassa*, homogalacturonan, pectins, rhamnogalacturonan, strawberry

Abbreviations: AFM, atomic force microscopy; APEL, antisense pectate lyase plants; APG, antisense polygalacturonase plants; HG, homogalacturonan; L_N, number-average contour length; L_W, weight-average contour length; PDI, polydispersity index; PG, polygalacturonase; PL, pectate lyase; RG, rhamnogalacturonan; XGA, xylogalacturonan.

1. Introduction

Pectins, polymers largely composed of galacturonic acid (GalA), are one of the major components of plant cell walls and probably the most complex structural polysaccharide in nature (Vincken et al., 2003). Polyuronides influence the physical and mechanical properties of the primary cell wall, fulfilling important biological functions during cell growth and development (Bacic, Harris & Stone, 1988; Bidhendi & Geitmann, 2016; Peaucelle et al., 2011). The middle lamellae between primary cell walls are also enriched in pectin, where it functions in regulating intercellular adhesion (Willats, McCartney, Mackie & Knox, 2001). Moreover, pectins have potential applications in areas such as the food industry and medicine, as a source of fibres and anticarcinogenesis products (Glinsky & Raz, 2009; Maxwell, Belshaw, Waldron & Morris, 2012).

Homogalacturonan (HG), a homopolymer of α-(1-4)-D-GalA which can be methylesterified at C-6 or acetylated at O-2 or O-3 is the most abundant polyuronide, accounting for 50-90% of most extracted pectins (Yapo, 2011). Rhamnogalacturonan II (RGII), xylogalacturonan (XGA) and other minority polymers, such as apiogalacturonan, galactogalacturonan and arabinogalacturonan, are often referred as substituted galacturonans due to the presence of a common galacturonan backbone (Ridley, O'Neill & Mohen, 2001; Yapo, 2011). RGII is composed of nine galacturonyl residues, containing clusters of four heteropolymeric side chains with more than 20 uncommon sugar residues and 20 different glycosidic linkages (O'Neill, Ishii, Albersheim & Darvill, 2004). RGII can dimerize by means of borate ester links, being dimeric Rhamnogalacturonan II the predominant form *in muro* (Yapo, 2011). XGA is a linear HG partially substituted at O-3 positions with single residues of xylose and/or small, 2-8 residues, β-D-Xyl side chains. XGAs are frequently found in storage tissues of reproductive organs (Yapo, 2011). Finally, rhamnogalacturonan I (RGI) polymers

76 are highly ramified pectins having a backbone of the repeating disaccharide [→2)-α-L-
77 Rhap-(1→4)-α-D-GalpA-(1→], partly substituted at O-4 or O-3 positions of rhamnose
78 (Rha) residues by arabinan, galactan and arabinogalactan side chains (Willats et al.,
79 2001; Yapo, 2011).

80 Although the chemical composition of pectins is well known, the way in which
81 these domains are inter-connected within the cell wall is unclear. Fig. 1 shows the
82 alternative models for pectin assembly that have been proposed. The most accepted
83 model shows the pectin composite as a linear backbone composed by HG (smooth
84 regions), that can be interspersed with rhamnosyl residues, alternated at regular
85 intervals with branched RGI, XGA, arabinan and arabinogalactan (hairy regions) (De
86 Vries, Rombouts, Voragen & Pilnik, 1982; Yapo, 2011) (Fig. 1A). The number of
87 residues in both regions varied in the range 75-120 for HG domains and 70-80 for RGI.
88 An alternative model postulates that RGI is the main pectin backbone, and linear HG
89 and XGA would be side chains of the RGI core (Vincken et al., 2003) (Fig. 1B). The
90 analysis of the oligomers obtained after acid hydrolysis of apple pectins performed by
91 Coenen, Bakx, Verhoef, Schols & Voragen (2007) partly supported the De Vries et al.
92 (1982) model, although the model where HG is positioned as a RGI side chain could
93 not be excluded. More recently, Yapo (2011) suggested a different model, in which the
94 pectin complex is formed by an RGI core, decorated with neutral sugars and XGA
95 side chains, connected with two unbranched HG blocks at the extremes (Fig. 1C).

96 Many methodological approaches from different scientific disciplines have been
97 used to characterize pectic polysaccharides. Pectins are complex heterogeneous
98 molecules and microscopic techniques, which can visualise individual molecules, are
99 ideal for characterizing such populations. Both transmission electron microscopy and
100 atomic force microscopy (AFM) provide suitable resolution and have been used to

101 study pectin molecules. AFM offers the advantages of imaging the molecules in a liquid
102 environment and of providing direct information on the height of the molecules: the
103 latter being particularly useful for ensuring single molecules are being studied and
104 allowing branching of the molecule backbone to be distinguished from overlapping of
105 molecules where the height would double at the crossover point (Kirby, Gunning &
106 Morris, 1996; Round, Rigby, MacDougall, Ring & Morris, 2001; Koziol, Cybulska,
107 Pieczywek & Zdunek, 2015). AFM has provided new information on the branching of
108 the pectin backbone; features such as contour length, branch length and distribution can
109 be studied through this technology (Round et al., 2001; Round, Rigby, MacDougall &
110 Morris, 2010; Morris, Gromer, Kirby, Bongaerts & Gunning, 2011). In general, AFM
111 studies of fruit pectins, independently of the species, show individual polymers,
112 unbranched or with a reduced number of long branches, which can be connected to
113 make up large fibres or micellar aggregates (Posé et al., 2012; Round et al., 2001;
114 Yang, Chen, An & Lai, 2009; Zareie, Gokmen & Javadipour, 2003). It has been
115 postulated that branches in linear chains are composed by HG, while neutral sugar are
116 present as much shorter chains, not detected by AFM (Round et al., 2001; Round et
117 al., 2010). The aggregates could represent or be remains of supramolecular pectin
118 structures present *in muro*. Along this line, Fishman, Chau, Cooke & Hotchkiss (2008)
119 observed strands and spherical particles integrated into networks in microwave-
120 extracted pectins isolated from sugar beet pulp. Pectin polymer lengths and the
121 number of aggregates diminish as the fruit ripen or during the postharvest storage
122 (Paniagua et al., 2014). More recently, Posé et al. (2015) used AFM to analyse pectins
123 isolated from strawberry fruits with a pecate lyase (PL) or a polygalacturonase (PG)
124 gene downregulated by antisense transformation, and they found a close relationship
125 between nanostructural complexity of polyuronides and fruit texture.

AFM has also provided new information on the nature of aggregated structures present in pectin extracts from the cell wall. In sodium carbonate soluble pectins from unripe tomato, Round, Rigby, MacDougall & Morris (2010) found that the release of neutral sugars by acid hydrolysis of the samples with 0.1 M HCl at 80ºC at different incubation times, did not affect individual pectin lengths but decreased the size of aggregates. These authors suggested that pectin aggregates were a mixture of RGI and HG, while isolated chains were composed of polygalacturonic acid. By contrast, Zhang, Cui, Xiao & Wang (2014), using a similar approach, observed a decrease in the length of individual pectin chains after acid hydrolysis of *C. edulis* and citrus peel, suggesting that these polymers contain RGI.

This study uses AFM to investigate further the structures of pectin samples from ripe native and mutant strawberry fruit. To this purpose, initially, we have analysed the effect of fungal endo-PG digestion in chain contour length and the number and size of aggregates in sodium carbonate soluble pectins from control and transgenic fruits with a PL or a PG gene downregulated. In addition, we used AFM to analyse pectins subjected to mild acid hydrolysis at 25ºC, a treatment that dissociates dimeric RGII complex into monomeric RGII (Kobayashi, Matoh & Azuma, 1996), to elucidate the role of RGII in the formation of the micellar aggregates.

2. Materials and methods

2.1. Plant material

Ripe strawberry (*Fragaria* × *ananassa,* Duch., cv. 'Chandler') fruits from control, non-transformed, plants and transgenic plants carrying antisense sequences of a pectate lyase gene, *FaplC* (line APEL39, described in Santiago-Doménech et al. (2008)), or a

polygalacturonase gene, *FaPG1* (line APG29, described in Posé et al. (2013)) were used as the source of pectins. Transgenic ripe fruits showed a strong reduction in *FaplC* or *FaPG1* mRNA levels, higher than 95% in both genotypes.

2.2. Cell wall isolation and pectin extraction

The procedure used for the isolation of the cell wall material from ripe strawberry fruits was based on the protocol of Redgwell, Melton & Brasch (1992) as modified by Santiago-Doménech et al. (2008). Briefly, 10-15 frozen fruits were ground to a powder in liquid N_2 and 20 g were homogenised in 40 ml of PAW (phenol: acetic acid: water, 2:1:1, w:v:v). The homogenate was centrifuged at 4000 *g* for 15 min and the supernatant filtered through Miracloth (Merck, Bioscience, UK). After centrifugation, the pellet obtained was treated with 90% aqueous DMSO to solubilise the starch. The extract was then centrifuged at 4000 *g* and the pellet washed twice with distilled water. The water fraction was discarded, and the de-starched pellet, which is considered the cell wall material, was lyophilised.

The cell wall material was fractionated as described previously (Santiago-Doménech et al., 2008) to obtain the Na_2CO_3 soluble pectin fraction. Briefly, cell wall material was washed overnight with deionised water, centrifuged at 6000 *g* for 15 min and the pellet was sequentially extracted with 0.05 M trans-1,2-diaminocyclohexane-N,N,N'N'-tetraacetic acid (CDTA) in 0.05 M sodium acetate buffer, pH 6, followed by 0.1 M Na_2CO_3 containing 0.1% $NaBH_4$. Sodium carbonate soluble fraction was exhaustively dialysed against distilled water and stored at -20ºC, as aqueous solution, until analysed by AFM. Galacturonic acid was determined by the carbazole method (Filisetti-Cozzi & Carpita, 1991), using galacturonic acid as standard.

176

177 *2.3. Endo Polygalacturonase digestion*

178 Pectin samples diluted to a concentration of 0.5 mg·ml^{-1} of GalA in 0.1 mM
179 ammonium bicarbonate buffer, pH 5.5, were digested with a diluted endo-PG (280
180 U/mg; E.C. 3.2.1.15; from *Aspergillus aculeatus*; Megazyme) at 40ºC (optimum
181 enzyme temperature recommended by the manufacturer). Enzymatic digestions were
182 stopped at 0, 1, 1.5, 2, 4, 6, 8 and 24 h by boiling the samples for 10 min. Different
183 dilutions of endo-PG were tested to avoid artefacts and interferences in the AFM
184 images. Samples incubated with buffer without enzyme were used as control. After
185 digestion, samples were visualized by AFM as described in the following sections.

186

187 *2.4. Acid hydrolysis treatment*

188 To determine the effect of dimeric RGII removal on pectin nanostucture, samples were
189 subjected to mild acid hydrolysis following the procedure of Kobayashi et al. (1996).
190 Samples (1 mg·ml^{-1}) were incubated in 0.1M HCl for 30 min at RT, neutralized with 1 N
191 NaOH and dialysed against pure water for 2 h. Then, samples were processed for AFM
192 visualization as described later. Non-treated samples and pectin samples treated with
193 water instead of 0.1 M HCl were used as controls.

194

195 *2.5. Atomic force microscopy*

196 AFM samples were prepared as described by Posé et al. (2012). Pectin samples were
197 diluted in water to a concentration of 2-4 µg·ml^{-1}. Then, 3 µl were pipetted onto freshly-
198 cleaved mica and dried over a heating block at 37 ºC. The sample was then inserted into
199 the liquid cell of the AFM microscope (manufactured by ECS, East Coast Scientific,
200 Cambridge, UK) and visualized under re-distilled butanol. Butanol was used as an

imaging solvent to limit desorption of the molecules from the substrate and to eliminate capillary condensation effects (Kirby et al., 1996; Round et al., 2001). Silicon nitride cantilevers for contact mode (Budget Sensors, Bulgaria) were used with a quoted force constant of 0.2 $N \cdot m^{-1}$. Samples, 1 μm^2 area, were scanned in contact mode at a frequency of 2 Hz. The use of butanol and the selected normal force minimise any distortion or disruption of the molecule. Fresh tips were used if deterioration observed. No noticeable differences in the widths of the molecules, or part of the molecules, were seen when observed parallel to or perpendicular to the scan direction, indicating a minor tip broadening effect. Images were collected and stored in both topographical and error signal mode. Topographical images were used for height measurements to identify individual molecules and branches and for calculations of the volume of the aggregates. The calibration of the AFM microscope was assessed with the calibration standard TGZ02 (NT-MDT Co. Building 167, Zelenograd, Moscow, 124460, Russia).

2.6. AFM image analysis

AFM files were converted to TIFF files using Paint Shop Pro v. 5.00 software and analysed offline. Individual molecules were defined as strands that were not entangled with, or overlapping other strands, and ones that lay entirely within the scanned area (Adams, Kroon, Williamson & Morris, 2003). Contour length of individual strands, defined as total length including backbone and branches, was analysed by plotting the length of the chains with the freehand tool of ImageJ software (Posé et al., 2012). The number-average (L_N) and the weight-average (L_W) contour lengths and their ratio (L_W/L_N) or polydispersity index (PDI) were calculated as described previously (Posé et al., 2012). The volumes of pectin aggregates were estimated using the image analysis software Gwyddion (2.40win32). The software estimates the volume between grain

surface and the basis surface formed by Laplacian interpolation of surrounding values. The molecular weights of the aggregates were calculated from these volumes using a galacturonic molecular weight of 176 Da, representing each monomer as a cylinder of 0.435 nm in length and 0.4 nm in radius, as described by Round et al. (2010). The number of aggregates per μm^2 was also recorded. Ten to 20 images per treatment were taken and 200-300 individual measurements from independent images were obtained to represent contour length distributions and to perform statistical analysis.

2.7. Statistical analysis

All experiments were performed by triplicate. The GraphPad Prism software (v.5.0 b) was used for statistical analyses. The medians from the original length distributions were compared by non-parametric Kruskal–Wallis test. Differences in the branching of the polymer chains, presence/absence of branches, were analysed by Chi-square test. The number of aggregates per μm^2 of sample was analysed by Mann Whitney U test. All statistical tests were performed at $P = 0.05$.

3. RESULTS

3.1. Effect of polygalacturonase digestion on nanostructure of sodium carbonate pectin samples

In this experiment, pectin samples were digested with fungal endo-PG during different times, and visualized by AFM. Initially, several endo-PG concentrations were tested to ensure that the final conditions chosen did not lead to artefacts due to the presence of the enzyme or the buffer used in the studies: a low enzyme

dilution, 1:10^5 (enzyme:water) corresponding to 0.13 U·mg^{-1} GalA in the assay, was found to not interfere with AFM images on the pectin extracts. Representative topographical AFM images of samples from Control fruits before and after enzymatic incubations are shown in Fig. 2, and those corresponding to APG and APEL samples in Supplementary Figs. 1 and 2, respectively. AFM images of pectin samples before treatment showed isolated chains, unbranched or with a small number of long branches, independently of the genotype. Additionally, larger tri-dimensional structures or micellar aggregates were also visible at lower frequency. These structures were characterized by entangled pectins in the centre with emerging chains, some of which were similar in size to isolated pectic chains. Images of the different structures visualized by AFM can be shown in Supplementary Fig. 3.

As a result of endo-PG treatment, a gradual decrease in the main backbone length of isolated chains as well as in the length of their branches was observed in the three samples. This was especially evident after 4h of endo-PG digestion (Fig. 2; Supplementary Figs. 1, 2 and 3). After this time, the number of linear chains that could be observed in the samples decreased significantly. Similarly, the number of micellar aggregates and their size decreased with the time of digestion. After 24 h of treatment, AFM images showed few filamentous structures and aggregates, independently of the genotype.

Supplementary Fig. 4 shows the contour length distributions of isolated pectic chains from the three genotypes at different digestion times. Pectin length varied in the range 10-400 nm with 50 and 75 nm being the more abundant contour length classes in the three genotypes before treatment. Endo-PG digestion shifted sample distributions to shorter chain length, with most polymers in the 0-25 nm class after 24h of digestion. The contour length distribution parameters number-average (L_N),

276 weight-average (L_W) and the polydispersity index (PDI) are shown in Table 1. The
277 medians (ME) of the original data were also included and used for statistical
278 comparison. Before enzymatic treatment, isolated chains from transgenic samples
279 were significantly larger than those present in controls. In all the samples, the
280 median of the length distributions decreased with the endo-PG incubation time, with
281 the differences in the initial ME values statistically significant after 1.5 h of digestion
282 in the case of Control and APG samples or 2 h in the case of APEL pectins. After 24 h
283 of enzymatic treatment, the three samples showed similar contour length parameters
284 despite APG and APEL chains being significantly larger than control chains before
285 digestion. The minimum polymer chain length reached after 24 h digestion was
286 around 22 nm. PDI index remained unchanged during the whole digestion process,
287 consistent with a process of random single depolymerisation events (Round et al.,
288 2010).

289 L_N data were fitted to an exponential decay curve using the equation

$$L_N = L_{N0} + a.e^{-bx}$$

290 being L_{N0} the minimum polymer chain length, a the difference between the maximum
291 L_N value and L_{N0}, and b a rate constant, expressed in units of h^{-1}, that indicates how
292 rapidly the curve descends. The three samples fitted well to this equation with R^2
293 values close to or higher than 0.9 (Fig. 3). As expected, a values were higher in
294 samples from both transgenic lines when compared with control pectins; however, L_{N0}
295 values were similar in the three samples. Interestingly, APEL pectins showed a lower
296 rate constant than the rest of genotypes. The half digestion time, calculated as $0.692/b$,
297 yielded values of 1.68, 1.65 and 2.47 h for control, APG and APEL samples,
298 respectively.

299 The percentage of branched polymer chains before PG treatment was around 6%

300 in control and APEL samples and significantly higher, >30%, in APG, as previously
301 described by Posé et al. (2015) (Supplementary Fig. 5). The level of branching
302 diminished after endo-PG treatment, and after 2 h of treatment no branched pectic
303 chains were observed in Control and APG samples (Supplementary Fig. 5). However,
304 APEL samples still maintained a low percentage of branched chains, which
305 disappeared after 4h of endo-PG digestion (Supplementary Fig. 5).
306 The volumes of the complexes were estimated according to Round et al. (2010)
307 and used to calculate number-average and weight-average molecular weights before
308 and after 24 h of endo-PG digestion (Table 2). Before digestion, Control and APEL
309 samples showed complexes of similar molecular weights and slightly higher than
310 those observed in APG samples; however, the medians of the distributions were not
311 statistically different. After PG digestion, size of complexes diminished significantly,
312 reaching similar values in the three sample pectins (Table 2).
313
314 *3.2. Effect of mild acid treatment on pectin structure*
315 To investigate the role of RGII in the nano-structure of linear chains and aggregates,
316 pectin samples from APG fruits were subjected to a mild acid hydrolysis treatment,
317 0.1M HCl for 30 min at room temperature, to split dimmers of RGII. APG samples
318 were used because their pectins displayed the highest number of aggregates. Fig. 4
319 shows a representative image of pectins prior to and after mild acid hydrolysis.
320 Apparently, the length of isolated pectic chains was unaffected, as well as the size of
321 aggregates. However, the number of aggregates that appeared in the AFM samples
322 was notably reduced, from a mean value of 6 complexes/μm^2 before hydrolysis to 1
323 complex/μm^2 after hydrolysis.
324 Isolated polymer chains were measured before and after acid hydrolysis and their

basic parameters calculated (Supplementary Table 1). Although L_N and L_W values decreased slightly after acid treatment, the medians of the length chain distributions were not statistically different. Similarly, the length of the branches as well as the percentage of branched molecules was not affected by the acid hydrolysis treatment (results not shown). The M_N and M_W molecular weights of the aggregates that remained in the AFM samples after the hydrolysis treatment were similar to those observed in non-treated samples (Supplementary Table 1).

4. DISCUSSION

4.1 Isolated chains and branches visualized by AFM are mainly formed by galacturonic acid

Mild acid hydrolysis (0.1M HCl, 80ºC) of pectins at different times in combination with AFM has been used in previous investigations to determine the structure of polyuronides and the association among HG and RGI in native cell walls (Round et al., 2010; Zhang et al., 2014). This treatment cleaves glycosidic linkages at different rates, i.e. arabinose and galactose are released very rapidly, followed by rhamnose with galacturonic acid being the most resistant (Thibault, Renard, Axelos, Roger & Crépeau, 1993). After 72 h hydrolysis, almost pure HG was recovered in the acid-insoluble fraction (Thibault et al., 1993). Round et al. (2010) found that the loss of neutral sugars during the hydrolysis of carbonate pectins extracted from unripe tomato did not have a significant effect either on pectin chain or branch length (Round et al., 2010), suggesting that isolated chains, including long branches, were formed solely by HG and not interrupted by RGI. According to these authors, RGI was located mainly in the micellar aggregates, since the size of these structures decreased during acid

hydrolysis. By contrast, Zhang et al. (2014) observed a reduction of lengths of main backbone and branch in alkali-soluble pectins from rhizomes of *Canna edulis* and citrus peel after hydrolysis, indicating that Rha was located at the backbone chain. These contrasting results could be related to a different composition and/or structure of the pectins analysed, as demonstrated by the amount of Rha that remained in the samples after 72h of hydrolysis, 66% of the initial Rha in *C. edulis* vs. traces of Rha in tomato pectins (Round et al., 2010; Zhang et al., 2014).

A different strategy to unravel the structure of fruit pectins has been followed in this study consisting in the analysis of samples by AFM after digestion with a fungal endo-PG at different times. Undigested strawberry ripe fruit pectins appeared mainly as linear chains, unbranched or with a low number of branches, and as micellar aggregates. The structure of these aggregates frequently includes strands emerging from the central core with sizes that are similar to those of isolated chains. Similar linear chains and aggregates have previously been described in pectin samples extracted from other fruits, e.g. tomato, peach, jujuba and apricot (Chen et al., 2013; Round et al., 2001; Wang et al., 2012; Yang et al., 2009). Endo-PGs catalyse the hydrolytic cleavage of α-(1-4) bonds between at least four de-methylesterified GalA residues of the HG backbone (Chen and Mort, 1996; Sénéchal, Wattier, Rustérucci & Pelloux, 2015). The digestion of strawberry pectins with fungal endo-PG reduced pectin chain length and eliminated pectin branches. Our results strongly support a galacturonic acid nature of linear strands and branches. The nature of the linkage involving GalA branches is unknown but several linkage analyses have found minor amounts of 2,4- and 3,4-linked galacturonosyl residues (Talmadge, Keegstra, Bauer & Albersheim, 1973; McNeil, Darvill & Albersheim, 1980; Peña & Carpita, 2004), which could represent branch points of the main pectin chain.

In spite of the large decrease in pectin backbone length due to endo-PG digestion, the pectin backbone was not totally degraded by the enzyme. In the three samples analysed, linear chains reached their minimum length after 8h of endo-PG treatment and no further reduction was observed at 24 h of treatment. Interestingly, the average size of the strands that remained at the end of the experiment, about 22 nm, was similar in the three genotypes despite the higher initial size of APG or APEL chains. The number of carbohydrate residues as well as molecular mass of the pectic structures visualized by AFM can be estimated from L_N values considering a 3_1 helical structure with a pitch of 1.34 nm, data obtained from fibre diffraction analysis of polygalacturonic acid by Walkinshaw & Arnott (1981). According to this approach, the degrees of polymerization of strawberry carbonate pectins before endo-PG digestion were 164, 215 and 205 for Control, APG and APEL fruits. The number of residues in the remaining chains after 24 h of endo-PG treatment was estimated around 52 residues, independently of the genotype. It has been proposed that essentially pure HG contains approximately 72-117 residues (Thibault et al., 1993; Yapo, 2011; Yapo, Lerouge, Thibault & Ralet, 2007). Interestingly, the number of residues digested by endo-PG fits within this range, 112 residues in the control genotype, suggesting that isolated polymers visualized by AFM are formed by a pure HG domain linked to a shorter polymer resistant to endo-PG digestion. In the transgenic genotypes, the silencing of the genes encoding pectinolitic enzymes could protect pectins from degradation in vivo, yielding chains of longer size.

As a first hypothesis, the endo-PG resistant fraction of the linear chains observed in this study might correspond to RGI. According to Yapo et al. (2007), RGI isolated backbone is about 70-80 residues, corresponding to 34-40 GalA-Rha disaccharide repeating units. This value is slightly higher than the number of residues found in the

400 strawberry polymers remaining after endo-PG treatment. Zhan, Janssen & Mort
401 (1998) observed that the digestion of commercial citrus pectins with endo-PG
402 produced two fractions: a predominant region of uninterrupted 1,4-linked GalA
403 residues, accounting for 80% by weight of the starting material, and a RGI region
404 containing neutral side chains. In this respect, the analysis of the oligomer fragments
405 released by acid hydrolysis of apple pectins indicated that both HG and XGA were
406 covalently linked to RGI, with RGI at the reducing end of the oligomer and HG/XGA
407 at the non-reducing end (Coenen et al., 2007). Interestingly, the absence of oligomers
408 with HG at the reducing-end suggested that the backbone of apple pectin consisted of
409 only one HG and one RGI structural element (Coenen et al., 2007). The putative
410 presence of RGI residues in the backbone of strawberry pectin chains is supported by
411 the observed reduction of pectin lengths after acid hydrolysis in *C. edulis* and citrus
412 (Zhang et al., 2014). However, this hypothesis does not match with the results of
413 Round et al. (2010) who found that chain length of tomato pectins was not altered
414 after 24h of acid hydrolysis despite the amount of Rha being almost totally depleted.
415 As an alternative explanation, the indigestible oligomer of the strawberry strands
416 could correspond to XGA. Xylogalacturonans are not degraded by endo-PGs.
417 Molecular weights of 20-30 kDa and a backbone minimum degree of polymerization
418 of 29-119 residues have been reported for XGA polymers (Yapo, 2011). However,
419 Posé et al. (2015) showed that the amount of xylose in strawberry pectins extracted
420 with sodium carbonate is half the amount of Rha. Further experiments are needed to
421 clarify this point. A hypothetical model for strawberry pectins based on the results
422 obtained in this research is shown in Fig. 1D.
423
424 *4.2 Aggregate complexes are partially degraded by fungal endo-PG and might be*

stabilized by dimeric RGII

Round et al. (2010) found that the acid hydrolysis of tomato pectins reduced size of aggregated complexes observed in the AFM samples from 965 to 453 kDa, suggesting that complexes contained RGI, HG chains and irreducible aggregates of HG. In our case, the number-average MW (M_N) of the complexes observed in the strawberry samples was in the range 900-1700 kDa, a value slightly higher than the one observed by Round et al. (2010) in tomato. After 24 h of endo-PG digestion, the number of complexes decreased as well as their MW, reaching a mean M_N value of 654 kDa. These results support the hypothesis of the complexes being partly composed of HG.

On the other hand, untreated samples from down-regulated *FaPG1* fruits showed a higher amount of aggregates than control and APEL samples, although their size were slightly lower. This result indicates that plant polygalacturonases may be involved in the disassembly of the tridimensional structure of these aggregates during fruit ripening. The smaller size of APG aggregates could explain the higher rate constant of endo-PG digestion of APG linear chains obtained in the kinetic plots when compared with APEL pectins. Linear chains from both APEL and APG samples were larger than control, and therefore a lower digestion rate constant, higher half digestion time, would be expected. This occurred for APEL samples but not for APG pectins. As the complexes are degraded simultaneously to the linear chains, new shorter chains might be liberated from the smaller APG complexes during the initial stages of endo-PG digestion and this would account for the lower half digestion time of these pectins when compared with APEL samples.

Despite RGII being a minor pectin component in the cell wall, it is believed that it could play an important role in the regulation of the pore size and other physical properties of the cell wall (O'Neill et al., 2004). In the traditional pectin model of

alternating “smooth” and “hairy” regions, RGII is integrated in the HG backbone. In the alternative pectin model proposed by Vincken et al. (2003), RGII domains are included in HG domains which are covalently cross-linked to RGI. Additionally, RGII can cross-link by borate-diol ester two HG domains (Vincken et al., 2003). Yapo (2011) proposed that the formation of RGII dimers is a prerequisite for pectin macromolecular formation. This molecule is able to form dimers via borate diester bridges between RGII molecules belonging to two different layers of pectins and also between pectic molecules within the same layer. Kobayashi et al. (1996) suggested the use of mild acid hydrolysis at room temperature for a short time (30 min) to break borate ester cross-linking without altering glycosidic linkages. The use of this treatment in strawberry pectins diminished in an 80% the number of aggregates, without altering the length of isolated chains or the branch pattern. Moreover, the volume of the aggregates that remain after treatment did not change. These results indicate that dimeric RGII could be a key component of micellar aggregates and part of their three-dimensional structure.

5. CONCLUSIONS

The enzymatic treatment of sodium carbonate soluble pectins from strawberry fruits with fungal endo-PG decreased the length of pectin chains and the number of branches. However, these single molecules were not completely degraded and a minimum pectin length of 22 nm, corresponding to about 52 residues, was reached after 8 h of digestion. It is noteworthy that the size of the chain that was degraded is in good agreement with the size of pure HG obtained by different methods (Morris, Ralet, Bonnin, Thibault & Harding, 2010; Thibault et al., 1993; Yapo et al., 2007). The existence of an endo-PG resistant unit as structural component of the linear chains was a reliable result, i.e. the results shown in the present study indicate that pectins from transgenic fruits with

475 pectinase genes silenced were significantly larger than control but the endo-PG digestion
476 of these samples also yielded polymers of around 22 nm. These results suggest that linear
477 polymers observed by AFM are a mixture of HG and more complex molecules composed
478 of a HG unit linked to a different polymer, likely RGI although the nature of this
479 component is speculative. On the other hand, the pectin complexes observed in AFM
480 samples were partially degraded by endo-PG treatment, indicating that these structures
481 also contain HG, as suggested by Round et al. (2010). Contrary to endo-PG treatment,
482 hydrolysis with diluted HCl at room temperature did not modify the length of pectin
483 strands, but significantly diminished the presence of aggregates. This treatment breaks
484 borate diester bonds between RGII, and therefore, our results indicate that RGII has a key
485 role in the formation and/or stabilization of these complexes. Based on these results, a
486 new hypothetical model for strawberry pectin assembly is proposed (Fig. 1D) in
487 which the pectin chains are formed by HG, unbranched or with a low number of HG
488 branches, and more complex molecules formed by a single HG unit linked to a RGI
489 unit. RGII would be located in the HG backbone or HG branches allowing the
490 formation of pectin aggregates through borate diester bridges between adjacent RGII
491 from different pectin molecules.
492
493 **Acknowledgements:** This work was supported by the Ministerio de Economía y
494 Competitividad of Spain and FEDER EU Funds (grant references AGL2011-24814 and
495 AGL2014-55784-C2-1-R) and by a Ramón y Cajal project RYC-2011-08839 awarded
496 to AJM. The use of AFM was supported by the Biotechnology and Biological Science
497 Research Council (BBSRC) through its core strategic grant to IFR.
498
499 **References**

Adams, E. L., Kroon, P. A., Williamson, G., & Morris, V. J. (2003). Characterisation of heterogeneous arabinoxylans by direct imaging of individual molecules by atomic force microscopy. *Carbohydrate Research*, *338*, 771-780.

Bacic, A,, Harris, P. J., & Stone, B. A. (1988). Structure and function of plant cell walls. In J. Preiss J (Ed.), *The Biochemistry of Plants,* (pp. 297–371). New York: Academic Press.

Bidhendi, A. J., & Geitmann, A. (2016). Relating the mechanics of the primary plant cell wall to morphogenesis. *Journal of Experimental Botany*, *67*, 449-461.

Coenen, G. J., Bakx, E. J., Verhoef, R. P., Schols, H. A., & Voragen, A. G. J. (2007). Identification of the connecting linkage between homo- or xylogalacturonan and rhamnogalacturonan type I. *Carbohydrate Polymers*, *70*, 224-235.

Chen, E. M. W., & Mort, J. A. (1996). Nature of sites hydrolyzable by endopolygalacturonase in partially-esterified homogalacturonans. *Carbohydrate Polymers, 29*, 129-136.

Chen, Y., Chen, F., Lai, S, Yang, H., Liu, H., Liu, K., Bu, G., & Deng, Y. (2013). In vitro study of the interaction between pectinase and chelate-soluble pectin in postharvest apricot fruits. *European Food Research and Technology, 217*, 1438-2377.

De Vries, J. A., Rombouts, F. M., Voragen, A. G. J., & Pilnik, W. (1982). Enzymic degra- dation of apple pectins. *Carbohydrate Polymers*, *2*, 25-33.

Filisetti-Cozzi, T. M. C. C., & Carpita, N. C. (1991). Measurement of Uranic Acids without interference from neutral sugars. *Analytical Biochemistry, 197*,157-162.

Fishman, M. L., Chau, H. K., Cooke, P. H., & Hotchkiss Jr., A. T. (2008). Global structure of microwave-assisted flash-extracted sugar beet pectin. *Journal of Agricultural and Food Chemistry, 56*, 1471-1478.

Glinsky, V. V., & Raz, A. (2009). Modified citrus pectin anti-metastatic properties: one

525 bullet, multiple targets. *Carbohydrate Research, 344*, 1788-1791.
526 Kirby, A. R., Gunning, A. P., & Morris, V.J. (1996). Imaging polysaccharides by
527 atomic force microscopy. *Biopolymers, 38*, 355-366.
528 Kobayashi, M., Matoh, T., & Azuma, J. (1996). Two chains of rhamnogalacturonan II
529 are cross-linked by borate-diol ester bonds in higher plant cell walls. *Plant*
530 *Physiology*, *110*, 1017-1020.
531 Koziol, A., Cybulska, J., Pieczywek, P. M., & Zdunek, A. (2015). Evaluation of
532 structure and assembly of xyloglucan from tamarind seed (*Tamarindus indica* L.)
533 with atomic force microscopy. *Food Biophysics, 10*, 396-402.
534 Maxwell, E. G., Belshaw, N. J., Waldron, K. W., & Morris, V. J. (2012). Pectin: An
535 emerging new bioactive food polysaccharide. *Trends in Food Science and*
536 *Technology*, *24*, 64-73.
537 McNeil, M., Darvill, A. G., & Albersheim, P. (1980) Structure of plant cell walls. X.
538 Rhamnogalacturonan I, structurally complex pectic polysaccharide in the walls of
539 suspension-cultured sycamore cells. *Plant Physiology, 66*, 1128-11234.
540 Morris, G. A., Ralet, M. -C., Bonnin, E., Thibault, J. -F., & Harding, S. E. (2010)
541 Physical characterization of the rhamnogalacturonan and homogalacturonan
542 fractions of sugar beet (*Beta vulgaris*) pectin. *Carbohydrate Polymers*, *82*, 1161-
543 1167.
544 Morris, V J. Gromer, A, Kirby, A. R, Bongaerts, R. J. M. & Gunning, A. P. (2011) Using
545 AFM and force spectroscopy to determine pectin structure and (bio) functionality
546 *Food Hydrocolloids, 25*, 230-23.
547 O'Neill, M. A., Ishii, T., Albersheim, P., & Darvill, A.G. (2004). Rhamnogalacturonan
548 II: structure and function of a borate cross-linked cell wall pectic polysaccharide.
549 *Annual Review of Plant Biology, 55*,109-139

550 Paniagua, C., Posé, S., Morris, V. J., Kirby, A. R., Quesada, M. A., & Mercado, J. A.
551 (2014). Fruit softening and pectin disassembly: an overview of nanostructural pectin
552 modifications assessed by atomic force microscopy. *Annals of Botany, 114*, 1375-
553 1383.
554 Peaucelle, A., Braybrook, S. A., Le Guillou, L., Bron, E., Kuhlemeier, C., & Höfte, H.
555 (2011). Pectin-induced changes in cell wall mechanics underlie organ initiation in
556 *Arabidopsis*. *Current Biology*, *21*, 1720-1726.
557 Peña, M. J., & Carpita, N. C. (2004). Loss of highly branched arabinans and
558 debranching of rhamnogalacturonan I accompany loss of firm texture and cell
559 separation during prolonged storage of apple. *Plant Physiology, 135*, 1305-1313.
560 Posé, S., Kirby, A. R., Mercado, J. A., Morris, V. J., & Quesada, M. A. (2012).
561 Structural characterization of cell wall pectin fractions in ripe strawberry fruits
562 using AFM. *Carbohydrate Polymers*, *88*, 882-890.
563 Posé, S., Paniagua, C., Cifuentes, M., Blanco-Portales, R., Quesada, M. A., &
564 Mercado, J. A. (2013). Insights into the effects of polygalacturonase *FaPG1* gene
565 silencing on pectin matrix disassembly, enhanced tissue integrity, and firmness in
566 ripe strawberry fruits. *Journal of Experimental Botany*, *64*, 3803-3815.
567 Posé, S., Kirby, A. R., Paniagua, C., Waldron, K. W., Morris, V. J., Quesada, M. A., &
568 Mercado, J. A. (2015). The nanostructural characterization of strawberry pectins
569 in pectate lyase or polygalacturonase silenced fruits elucidates their role in
570 softening. *Carbohydrate Polymers*, *132*, 134-145.
571 Redgwell, R. J., Melton, L. D., & Brasch, D.J. (1992), Cell wall dissolution in
572 ripening kiwifruit (*Actinidia deliciosa*): solubilization of the pectic polymers.
573 *Plant Physiology, 98*,71–81.
574 Ridley, B. L., O'Neill, M. A., & Mohnen, D. (2001). Pectins: Structure, biosynthesis,

and oligogalacturonide-related signaling. *Phytochemistry, 57*, 929-967.

Round, A. N., Rigby, N. M., MacDougall, A. J., Ring, S. G., & Morris, J. V. (2001). Investigating the nature of branching in pectin by atomic force microscopy and carbohydrate analysis. *Carbohydrate Research, 331*, 337-342.

Round, A. N., Rigby, N. M., MacDougall, A. J., & Morris, V. J. (2010). A new view of pectin structure revealed by acid hydrolysis and atomic force microscopy. *Carbohydrate Research*, *345*,487-497.

Santiago-Doménech, N., Jiménez-Bemúdez, S., Matas, A. J., Rose, J. K. C., Muñoz-Blanco, J., Mercado, J. A., & Quesada, M. A. (2008). Antisense inhibition of a pectate lyase gene supports a role for pectin depolymerization in strawberry fruit softening. *Journal of Experimental Botany*, *59*, 2769-2779.

Sénéchal, F., Wattier, C., Rustérucci, C., & Pelloux, J. (2014), Homogalacturonan modifying enzymes: structure, expression, and roles in plants. *Journal of Experimental Botany, 65*, 5125-5160.

Talmadge, K. W., Keegstra, K., Bauer, W. D. & Albersheim, P. (1973) The structure of plant cell walls. I. The macromolecular components of the walls of suspension-cultured sycamore cells with a detailed analysis of the pectin polysaccharides. *Plant Physiology, 51*, 158-173.

Thibault, J. -F., Renard, C. M. G. C., Axelos, M. A. V., Roger, P., & Crépeau, M.-J. (1993). Studies of the length of homogalacturonic regions in pectins by acid hydrolysis. *Carbohydrate Research*, *238*, 271-286.

Vincken, J., Schols, H. A., Oomen, R. J. F. J., McCann, M. C., Ulvskov, P., Voragen, A. G. J., & Visser, R. G. F. (2003). If homogalacturonan were a side chain of Rhamnogalacturonan I. Implications for cell wall architecture. *Plant Physiology, 132*, 1781-1789.

600 Walkinshaw, M. D., & Arnott, S. (1981). Conformations and interactions of pectins. I.
601 X-ray diffraction analyses of sodium pectate in neutral and acidified forms. *Journal*
602 *of Molecular Biology*, *153*, 1055-1074.
603 Wang, H., Chen, F., Yang, H., Chen, Y., Zhang, L., & An, H. (2012). Effects of
604 ripening stage and cultivar on physicochemical properties and pectin
605 nanostructure of jujubes. *Carbohydrate Polymers*, *89*, 1180-1188.
606 Willats, W. G. T., McCartney, L., Mackie, W., & Knox, J. P. (2001). Pectin: cell
607 biology and prospects for functional analysis. *Plant Molecular Biology*, *47*, 9-27.
608 Yang, H., Chen, F., An, H., & Lai, S. (2009). Comparative studies on nanostructures of
609 three kinds of pectins in two peach cultivars using atomic force microscopy.
610 *Postharvest Biology and Technology, 51*,391-398.
611 Yapo, B. M. (2011). Pectic substances: from simple pectic polysaccharides to complex
612 pectins - A new hypothetical model. *Carbohydrate Polymers, 86*, 373-385.
613 Yapo, B. M., Lerouge, P., Thibault, J. -F., & Ralet, M. -C. (2007). Pectins from citrus
614 peel cell walls contain homogalacturonans homogeneous with respect to molar
615 mass, rhamnogalacturonan I and rhamnogalacturonan II. *Carbohydrate Polymers*,
616 *69*, 426-435.
617 Zareie, M. H., Gokmen, V., & Javadipour, I. (2003). Investigating network, branching,
618 gelation and enzymatic degradation in pectin by atomic force microscopy. *Journal*
619 *of Food Science and Technology*, *40*, 169-172.
620 Zhang, J., Cui, J, Xiao, L., & Wang, Z. (2014). The combination of atomic force
621 microscopy and sugar analysis to evaluate alkali-soluble *Canna edulis* Ker pectin.
622 *Food Chemistry*, *156*, 64-71
623

624 **Table 1.** Descriptors of contour length distributions of sodium carbonate soluble
625 pectins extracted from ripe strawberry fruits from control, APG and APEL lines at
626 different times of digestion with endo-PG. L_N: number-average, L_W: weight-average,
627 PDI: L_W/L_N ratio, ME: median values of the original data. ME values with different
628 letters are significantly different by non-parametric Kruskal–Wallis test at P=0.05.
629 Capital letters for comparison among genotypes in columns and lower letters for
630 comparison among the different digestion times within each genotype.

		Digestion time (hours)							
		0	1	1.5	2	4	6	8	24
Control	L_N (nm)	73.2	65.3	46.6	40.8	33.7	28.9	20.2	25.2
	L_W (nm)	88.3	86.9	61.2	50.0	49.4	38.2	30.2	33.1
	PDI	1.2	1.3	1.3	1.2	1.5	1.3	1.5	1.3
	ME (nm)	64.6Ba	55.0Ca	39.1Cb	35.6Bb	29.3Bc	27.1Bc	20.2Bd	24.4Acd
APG	L_N (nm)	95.9	78.5	63.4	37.9	49.4	32.4	19.1	22.4
	L_W (nm)	126.1	96.5	87.0	48.5	68.3	45.3	25.4	30.1
	PDI	1.3	1.2	1.4	1.3	1.4	1.4	1.3	1.3
	ME (nm)	81.7Aa	71.1Bab	57.4Bbc	31.4Cd	41.9Acd	28.5Bde	22.9Bf	23.4Aef
APEL	L_N (nm)	91.4	87.9	78.0	54.9	39.2	38.4	33.8	22.9
	L_W (nm)	120.3	106.9	101.5	65.3	55.3	50.7	44.4	30.8
	PDI	1.3	1.2	1.3	1.2	1.4	1.3	1.3	1.3
	ME (nm)	81.7Aa	82.2Aa	72.6Aab	51.7Ab	33.4Bc	33.4Ac	31.0Acd	22.4Ad

631

632

633 **Table 2.** Molecular weights of aggregates from control, APG and APEL pectin
634 samples after digestion with endo-PG. M_N: number-average, M_W: weight-average,
635 PDI: ratio M_W/M_N, ME: median values of the original data. ME values with different
636 letters are significantly different by non-parametric Kruskal–Wallis test at P=0.05.
637 Capital letters for comparison among genotypes in columns and lower letters for
638 comparison between 0 and 24 hours within each genotype.

Aggregates		Digestion time (hours)	
		0	24
Control	M_N (kDa)	1690.3	618.7
	M_W (kDa)	2727.8	886.4
	PDI	1.6	1.4
	ME (kDa)	1406.4Aa	503.8Ab
APG	M_N (kDa)	1170.0	703.1
	Mw (kDa)	1396.1	1223.3
	PDI	1.2	1.7
	ME (kDa)	960.0Aa	571.4Ab
APEL	M_N (kDa)	1755.0	641.7
	Mw (kDa)	2863.8	928.8
	PDI	1.6	1.4
	ME (kDa)	1331.2Aa	469.4Ab

639

640

Figures

Fig. 1: Schematic diagrams of the structural models for pectin assembly. (A). Classical model depicting the pectin backbone as an extended chain with HG (smooth) and RGI (hairy) regions (De Vries et al., 1982). (B). An alternative model showing pectin formed by a RGI backbone containing neutral polymers, HG and XGA side chains (Vincken et al., 2003). (C). Model proposed by Yapo (2011) in which the pectin complex is formed by a RGI core connected with two unbranched HG blocks at the extremes. Neutral polymers, XGA and other HG blocks are side chains of the RGI core. (D). Hypothetical strawberry pectin structure deduced from the results obtained in this research. Linear pectin chains observed by AFM would be a mixture of HG chains and complex molecules formed by a HG domain of about 110 residues linked to a RGI core (52 residues). The HG unit is unbranched or contains a few number of HG branches. RGII could be linked to the HG unit allowing the formation of pectin aggregates through borate diester bridges between adjacent RGII from different pectic molecules. dp: degree of polymerization.

Fig. 2: Representative topographical AFM images of sodium carbonate soluble pectins from cell wall extracts of ripe control fruits incubated with endo-PG at different time intervals. Arrows indicate pectin complexes. Figure contrast was automatically adjusted with the software Gwyddion for a better visualization. The scale bars correspond to 100 nm.

Fig. 3: Representation of the number average (L_N) of linear chains at different endo-PG digestion times. The curves corresponds to the adjustment of the data to an exponential decay curve using the equation $L_N = L_{N0} + a.e^{-bx}$, being L_{N0} the minimum polymer chain length, a the difference between the maximum L_N value and L_{N0}, and b a rate constant.

Fig. 4: Representative error mode (A, B) and topographical (C, D) AFM images of sodium carbonate soluble pectins from cell wall extracts of ripe APG fruits before (A, C) and after hydrolysis with 0.1M HCl for 30 min at RT (B, D). Arrows indicate pectin complexes. The scale bars correspond to 100 nm.

Supplementary material

Supplementary Table 1. Descriptors of contour length distributions of linear pectin chains and aggregates extracted from ripe APG strawberry fruits after mild hydrolysis with 0.1M HCl at room temperature for 30 min. L_N, M_N: number-average, L_W, M_W: weight-average, PDI: L_W/L_N ratio, ME: median values of the original data. ME values with different letters are significantly different by the Median test at P=0.05.

Supplementary Fig. 1: Representative topographical AFM images of sodium carbonate soluble pectins from cell wall extracts of ripe APG fruits incubated with endo-PG at different time intervals. Figure contrast was automatically adjusted with the software Gwyddion for a better visualization. The scale bars correspond to 100 nm.

Supplementary Fig. 2: Representative topographical AFM images of sodium carbonate soluble pectins from cell wall extracts of ripe APEL fruits incubated with endo-PG at different time intervals. Figure contrast was automatically adjusted with the software Gwyddion for a better visualization. The scale bars correspond to 100 nm.

Supplementary Fig. 3: Detailed images of linear chains and aggregates observed in AFM samples of strawberry pectins. (A) Branched chains before digestion with endo-PG. (B) Linear chains after 4 h of digestion with endo-PG. (C) Micellar aggregates before digestion with endo-PG showing entangled pectins in the centre with emerging chains. (D) Aspect of aggregates after digestion with endo-PG, showing a reduction in complex volume and the almost disappearance of the emerging chains.

Supplementary Fig. 4: Contour length distribution of sodium carbonate soluble polymers isolated from fruit cell walls of control, APG and APEL ripe fruits. Bars represent relative frequencies of the observed data.

Supplementary Fig. 5: Percentages of branched polymer chains after digestion with endo-PG at different time intervals.

Figure 1

Click here to download high resolution image

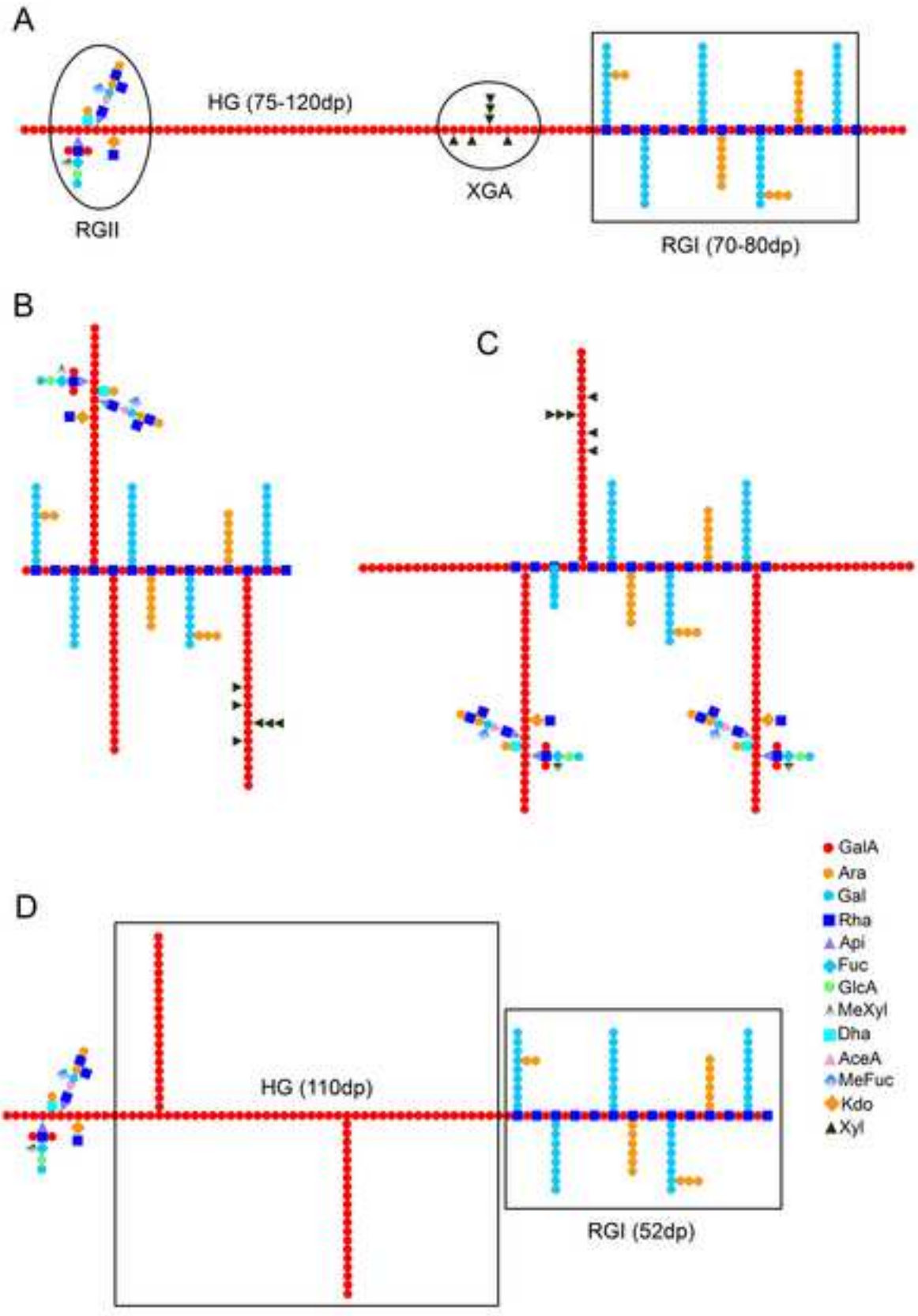

Figure 2

Click here to download Figure(s): Fig_2_New.ppt

Figure 2: Representative topographical AFM images of sodium carbonate soluble pectins from cell wall extracts of ripe control fruits incubated with endo-PG at different time intervals. Arrows indicate pectin complexes. Figure contrast was automatically adjusted with the software Gwyddion for a better visualization. The scale bars correspond to 100nm.

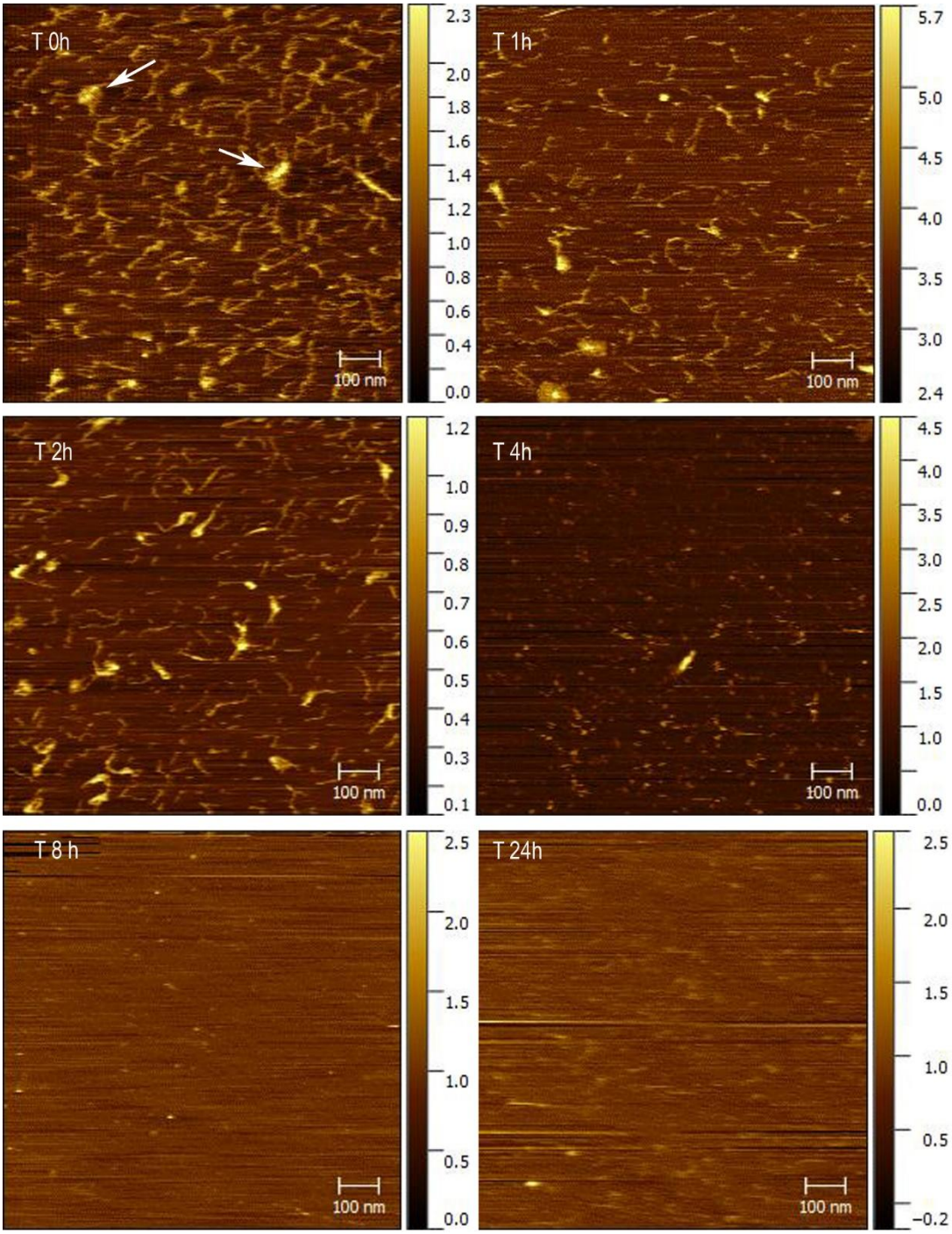

Figure 3

Click here to download Figure(s): Fig_3.ppt

Fig. 3: Representation of the number average (L_N) of linear chains at different endo-PG digestion times. The curves corresponds to the adjustment of the data to an exponential decay curve using the equation $L_N = L_{N0} + a.e^{-bx}$, being L_{N0} the minimum polymer chain length, a the difference between the maximum L_N value and L_{N0}, and b a rate constant.

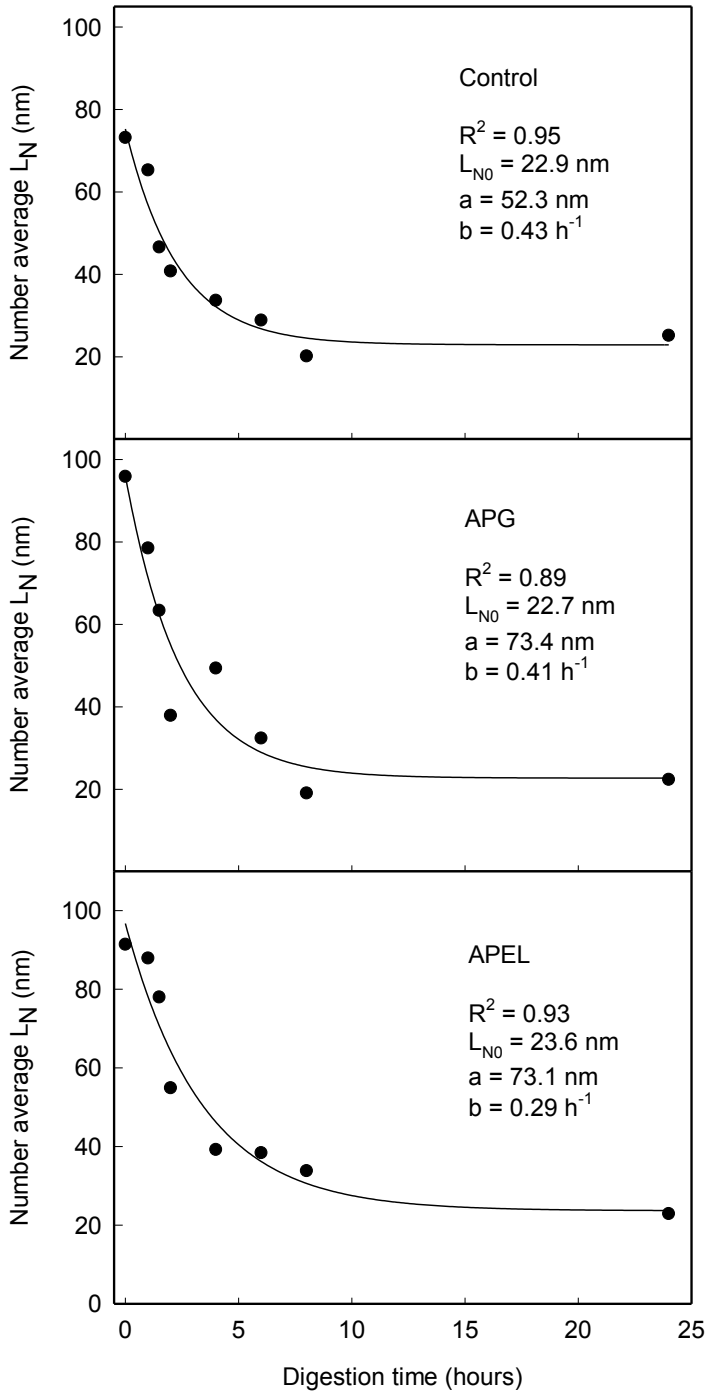

Figure 4

Click here to download Figure(s): Fig_4.ppt

Fig. 4: Representative error mode (A, B) and topographical (C, D) AFM images of sodium carbonate soluble pectins from cell wall extracts of ripe APG fruits before (A, C) and after hydrolysis with 0.1M HCl for 30min at RT (B, D). Arrows indicate pectin complexes. The scale bars correspond to 100nm.

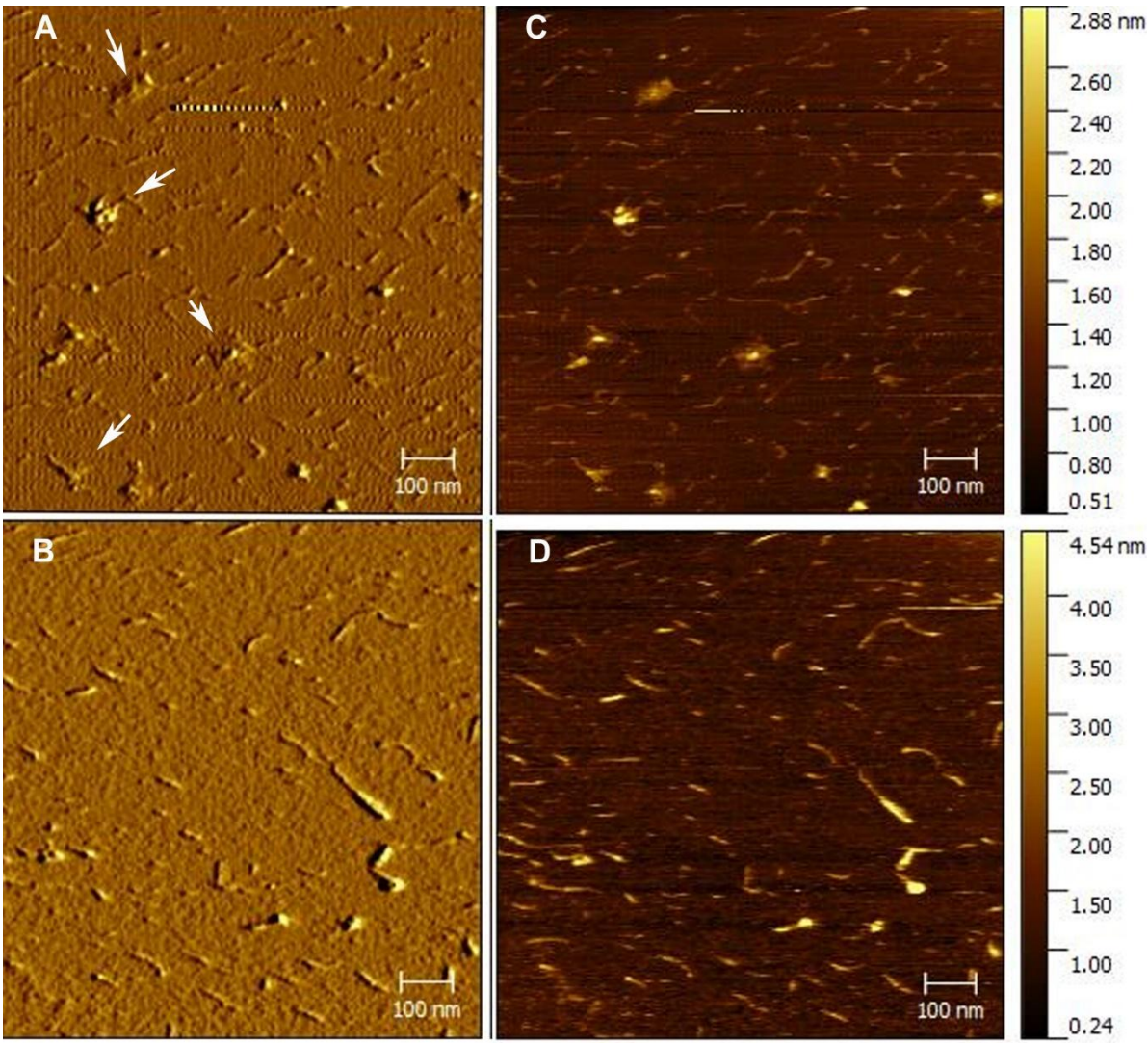

Supplementary Material

Click here to download Supplementary Material: Supplementary material-revised.pdf